

Quark-Hadron Duality in the 't Hooft Model for Meson Weak Decays: Different Quark Diagram Topologies

Benjamín Grinstein*

Department of Physics, University of California at San Diego, La Jolla, CA 92093

Richard F. Lebed†

Jefferson Lab, 12000 Jefferson Avenue, Newport News, VA 23606

(May, 1998)

Abstract

We compare the effects of different quark diagram topologies on the weak hadronic width of heavy-light mesons in the large N_c limit. We enumerate the various topologies and show that the only one dominant (or even comparable) in powers of N_c to the noninteracting spectator “tree” diagram is the “annihilation” diagram, in which the valence quark-antiquark pair annihilate weakly. We compute the amplitude for this diagram in the 't Hooft model (QCD in 1+1 spacetime dimensions with a large number of colors N_c) at the hadronic level and compare to the Born term partonic level. We find that quark-hadron duality is not well satisfied, even after the application of a smearing procedure to the hadronic result. A number of interesting subtleties absent from the tree diagram case arise in the annihilation diagram case, and are described in detail.

11.10.Kk, 11.15.Pg, 13.25-k

Typeset using REVTeX

*bgrinstein@ucsd.edu

†lebed@jlab.org

I. DESCRIPTION OF THE PROBLEM

The notorious difficulty of computing strong interaction quantities from first principles leads directly to a multitude of models, methods, and approximations. QCD lore dictates that inclusive rates, *i.e.*, those for which we do not inquire about any detail of the final hadronic state, are given to good approximation by the corresponding rate in a theoretical world of unconfined, perturbative final-state quarks. This lore, known as “quark-hadron duality” is seldom shown to follow from first principles. In some cases, such as the rate of $e^+e^- \rightarrow$ hadrons, an operator product expansion can be used to demonstrate the lore for quantities in which one averages over the energy of the final-state hadronic system. This is the so-called “global” duality, in contrast to duality for unaveraged quantities, or “local” duality.

Quark-hadron duality applied to decays of heavy mesons permits the computation of many important quantities, such as meson lifetimes, hadronic branching fractions, and the average number of charm quarks per beauty quark decay. One must note that the duality used here is of the “local” variety, and therefore less likely to be valid. Indeed, the sizeable deviations between theoretical predictions utilizing this form of duality and experiment for lifetimes, branching fractions and charm countings suggest that either there are large corrections to duality, or worse, that the duality lore simply does not apply in this context.

In this paper we study whether duality holds for annihilation decays of heavy mesons in a highly simplified but soluble strongly interacting theory; in a previous paper [1] we explored this issue for spectator decays of heavy mesons. We also investigate the validity of duality in the interference between spectator and annihilation decays.

To inquire about duality in a model, one must require that the model exhibits permanent quark confinement and asymptotic freedom; the former is necessary for a meaningful definition of purely hadronic properties, while the latter is believed to be the main ingredient of duality. The 't Hooft model is a good candidate: It satisfies these requirements and behaves, in many other respects, much like the real world of strong interactions.

Perhaps still the most straightforward and frequently used model of strong interactions is the constituent quark model, in which hadrons are envisioned as consisting of confined but otherwise weakly interacting valence quarks. Although deep inelastic scattering experiments clearly show that the true structure of a hadron incorporates a much more complicated brew of gluons and sea quarks, the undeniable success of the quark model in predicting hadronic spectra or enumerating decay modes still leads researchers to apply this scheme immediately when approaching a new hadronic system.

The asymptotically free parton result, *i.e.*, the result of the valence quark model dressed with perturbative QCD corrections, is also the leading term in an Operator Product Expansion [2] (OPE), in those cases where an OPE is known to exist, such as deep inelastic lepton-hadron scattering [3] and e^+e^- annihilation [4], as well as semileptonic processes involving heavy quarks [5]. One feature held in common by these processes is the presence of a large mass or energy scale, which provides the inverse expansion parameter of the OPE; consequently, it is tempting to suppose that other processes with large scales also possess OPEs. Such is the case for the nonleptonic decays of B mesons, where an OPE in powers of $1/m_b$ is purported to exist [6].

As of the time of this writing, measurements of many of these exclusive channels at

CLEO and LEP are being performed for the first time. Apart from the intrinsic value of such information, nonleptonic B decays are expected to provide valuable insights into QCD, magnitudes of CKM elements, and CP violation; consequently, understanding these decays has become the focus of much recent theoretical work. But the theoretical situation is wide open, precisely because no part of the decay is free of the complications of strong interaction physics.

When applied to a \bar{B} meson, the lore of quark model calculations or the expansion of Ref. [6] declares that the inclusive decay width should be dominated by the (color-unsuppressed) “tree” diagram T (Fig. 1), in which the b quark decays to a lighter flavor by emission of a W^- , particularly as $m_b \rightarrow \infty$. The daughter quark of the b then combines with the spectator antiquark to form one meson, whereas the quark-antiquark pair from the nonleptonic decay of the W form another. The above process assumes factorization, which means that the W system and daughter-spectator systems are regarded as non-interacting after the initial weak vertex. One very interesting comparison that can be made at this point is between the width obtained by the sum of such diagrams in Fig. 1 regarded as hadronic decays and the corresponding free quark decay.

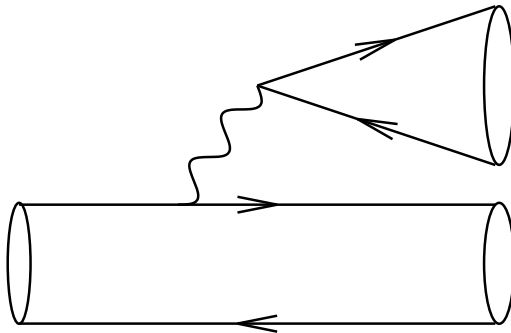


FIG. 1. The (color-unsuppressed) “tree” (T) parton diagram for the decay of one meson into two mesons. Ovals indicate the binding of partons into hadrons.

Of course, such a diagram is but one possibility, even in the simple quark model. For example, the spectator antiquark and the antiquark from the W^- decay may trade places before hadronization, the “color-suppressed” tree diagram C (Fig. 2). Such an amplitude is suppressed by a factor of N_c , the number of QCD color charges, compared to the T amplitude, since the W is a color singlet; thus, the color indices are automatically suitable for creating colorless mesons in Fig. 1, but require rearrangement in Fig. 2. Of course, in a real meson there may be additional dynamical enhancements or suppressions, and moreover, the exchange of *any* number of gluons and color charge between the quarks on opposite sides of the W line may completely muddle the hierarchy based on large N_c counting.

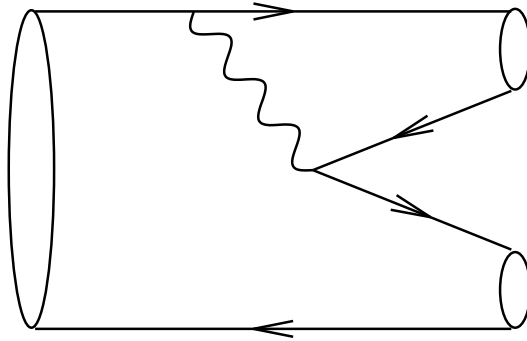


FIG. 2. The “color-suppressed” (C) parton diagram for the decay of one meson into two mesons. Ovals indicate the binding of partons into hadrons.

Likewise, the “annihilation” amplitude A (Fig. 3), in which the valence quark-antiquark pair of the \bar{B} annihilate to a W (quantum numbers permitting), is assumed to be suppressed compared to the T amplitude because of the difficulty of the b quark and the antiquark “finding” each other in the meson in order to annihilate. Quantitatively, this probability is proportional to the square of the meson wave function at vanishing quark separation, $|\psi(0)|^2 \propto f_B^2$ (the van Royen-Weisskopf relation). To compare this probability with that of the T diagram, one then argues that the only remaining dimensionful quantity that can be used to form a probability is m_B , so that the relative probability of an annihilation to a tree process is $f_B^2/m_B^2 \leq O(0.2\%)$.

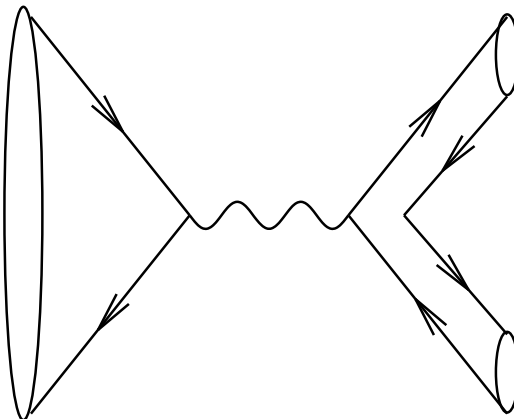


FIG. 3. The “annihilation” (A) parton diagram for the decay of one meson into two mesons. Ovals indicate the binding of partons into hadrons.

Nevertheless, other concerns lead one to believe that the annihilation and other non-spectator diagrams may be more important than one would naively expect. For, if non-interacting spectator diagrams dominate decays of b hadrons, how then does one explain the fact that the lifetime of \bar{B} mesons is greater than that of Λ_b baryons by 30% or more [7]? One possible explanation is that the naive estimate of the previous paragraph fails to include potentially large numerical coefficients. This point of view has been voiced recently in Ref. [8], in which it is suggested that the annihilation width has an unexpected additional enhancement of $16\pi^2$ compared to the tree width. One obtains this result by application of perturbative unitarity of the S-matrix to a cut across loop diagrams (Figs. 4a,b).

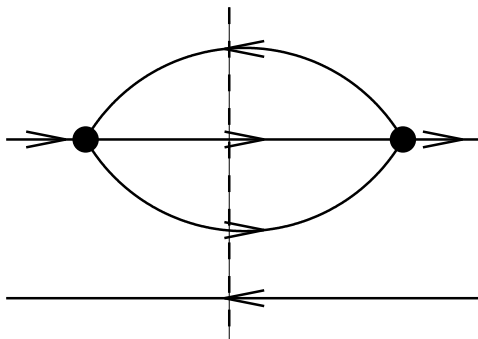


FIG. 4a. Diagram giving rise to the “tree” amplitude of Fig. 1 upon a vertical cut through the center (application of unitarity). The vertex blobs indicate W exchange.

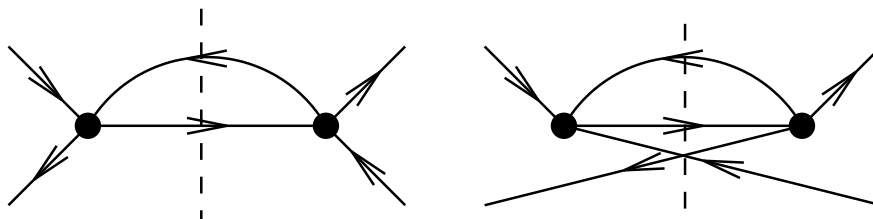


FIG. 4b. Diagrams giving rise to the “annihilation” amplitude of Fig. 3 upon a vertical cut through the center (application of unitarity). The vertex blobs indicate W exchange. Strongly produced $q\bar{q}$ pairs are not drawn here for simplicity.

Since the diagram giving rise to the tree width requires an additional loop integration compared to that for the annihilation width, the latter is enhanced by a relative factor of $16\pi^2$ (multiplied by the original factor f_B^2/m_B^2).

But is such an effect genuine? As soon as one includes the gluon lines necessary to bind real mesons, the counting of loops no longer leads to an obvious enhancement, unless we impose another hierarchy to suppress the effects of these exchanged gluons. The difficulty originates, as always, in our inability to take into account the multitude of gluons and virtual quarks involved in the strong coupling of mesons.

A question similar in spirit is that of the sense in which the partonic annihilation diagram Fig. 3 exhibits quark-hadron duality with its corresponding sum of exclusive hadronic channels. Just as it is expected that the width obtained from the tree diagram Fig. 1 approaches its corresponding sum of exclusives as the heavy quark mass becomes large, one may study whether this is true for processes in which the quantum numbers of the quarks are such that an annihilation diagram but not a tree diagram is permitted.

Unfortunately, the determination of definitive solutions to these questions requires one to have in hand exact solutions of QCD, and so is currently out of reach.

However, there does exist a simpler universe in which QCD can be solved exactly, so that we may consider the problem of meson decays in either quark or hadron language. As ’t Hooft showed long ago [9], the Green functions of QCD in one spatial and one time dimension (1+1) in the limit of $N_c \rightarrow \infty$ are completely calculable. Despite these large modifications from our universe, the ’t Hooft model remains a nontrivial theory that possesses the attractive feature of realizing confinement by binding quark-antiquark pairs into color-singlet mesons (and more generally, forbidding colored states [10]), as well as asymptotic freedom and the

many phenomenological results of large- N_c QCD [11] common to our $N_c = 3$ universe, such as dominance of scattering amplitudes by diagrams with a minimum of meson states, OZI suppression, the absence of exotics, and others [12].

In this paper we consider the analogue of \bar{B} weak nonleptonic decays in 1+1, where “ \bar{B} ” means a meson with a heavy quark (“ b ”) of mass M and a light antiquark of mass m ; “heavy” and “light” quark are terms made more precise in Sec. III. We studied the question of quark-hadron duality for the tree diagram in Ref. [1], in which it was shown that agreement between the two pictures as $M \rightarrow \infty$ occurred in a subtle and surprising manner with such high precision that the discrepancy between the two yielded a remarkable result: a correction to the Born term partonic limit well-fit numerically by a term of relative order $1/M$. Encouraged by this result, we ask what may be learned from other topologies of Feynman diagrams. We study in detail the annihilation diagram and compare the total width with that obtained from the parton model. Our motivation, as before, is the hope that the results from a soluble theory quite similar to real QCD in some respects and quite different in others may shed light on the full four-dimensional problem.

The paper is organized as follows. We begin in Sec. II with an enumeration of the various quark diagram topologies and study the scaling of each in the large N_c limit. This classification is independent of the number of spacetime dimensions. We find that, in the decays of interest, naive N_c power counting at the diagram level is subtle and deserves special discussion. The annihilation diagram emerges as the dominant topology and is the one whose computation is studied in the subsequent portion of the paper. In Sec. III, we briefly review the more arcane features of 1+1 dimensional physics and the ’t Hooft model that are particularly relevant to the subsequent calculations. Section IV exhibits the algebraic results of the inclusive parton-level calculation of widths, from both a naive tree-level diagram and an analysis based on loop diagrams as in Fig. 4b, the latter being related closely to the corresponding OPE-like expansion. In Sec. V, we present the results of the width calculation through exclusive hadronic channels in the ’t Hooft model. Section VI gives our numerical results and a discussion of their implications, and Sec. VII concludes. A short Appendix discusses the van Royen-Weisskopf relation in arbitrary dimensions.

II. QUARK DIAGRAM TOPOLOGIES AND LARGE N_C

In order to obtain Green functions for exclusive decays in the ’t Hooft model, one must first decide which diagrams are present at leading order in N_c . As is well known, n -meson couplings in large N_c appear with a suppression factor $N_c^{(1-n/2)}$, and therefore the leading meson decay diagrams are those producing only two final-state mesons. However, for some diagram topologies there is the possibility of direct oscillation of the \bar{B} meson into a single highly excited meson of the same mass. Such resonant production poses an interesting problem of large N_c counting, as we discuss below.

Next, we consider the relevant diagrams in terms of quarks, gluons, and electroweak bosons, in order to count factors of N_c appearing in these diagrams. To lowest order in electroweak coupling, a single gauge boson is required; moreover, since we require the decay of a quark, the boson must be a flavor-changing W rather than a γ or Z . It is convenient to classify all possible diagram topologies according to six classes given by Ref. [13], since these account for all possible diagrams including only one electroweak gauge boson. The

categories include the color-unsuppressed tree diagram T (Fig. 1), the color-suppressed tree diagram C (Fig. 2), the annihilation diagram A (Fig. 3), the electroweak “exchange” diagram E (Fig. 5a), the “penguin” diagram P (Fig. 5b), and the “penguin annihilation” diagram PA (Fig. 5c). For the P diagram exhibited in Fig. 5b it should be noted that the gluon may instead attach directly to the spectator antiquark, in which case production of an additional quark-antiquark pair is not required. Similarly, the PA topology includes diagrams in which the intermediate glue connects to a single final-state $q\bar{q}$ pair. Although these diagrams were originally exhibited in the context of quark model calculations, they suit our purposes since the inclusion of each additional meson, quark-antiquark pair, or external gluon is accompanied by suppressions in the amplitude of orders $1/\sqrt{N_c}$, $1/N_c$ and $1/\sqrt{N_c}$, respectively. Furthermore, diagrams with internal gluons are either nonplanar and hence suppressed by powers of $1/N_c^2$, or planar and produce a diagram at most of the same order in N_c as the diagram obtained when all such gluons are removed. Thus, the simple diagrams displayed in the figures are representatives of those with the leading behavior in N_c for each possible topology.

The electroweak gauge boson does not carry color charge, and so the possible diagrams fall into two categories: those in which the boson connects two otherwise disjoint color loops, and those in which the boson begins and ends on quarks already connected by gluons and therefore within a single color loop structure. Clearly, the former diagrams boast one extra color loop, and thus dominate the latter by a factor of N_c . The former set consists only of the T and A diagrams, whereas the latter set includes C, E, P, and PA diagrams. Only for T and A diagrams does the amplitude factorize into a product of a decay constant and the matrix element of a current between two mesons. Finally, forming a color-singlet meson for the one initial and two final mesons brings in a factor of $N_c^{-3/2}$ for each amplitude, and so we find that the amplitude is $\propto N_c^{+1/2}$ for T and A, $\propto N_c^{-1/2}$ for C, E, and P, and $\propto N_c^{-3/2}$ for PA. Widths are obtained by squaring the amplitudes and folding in phase space as usual, which adds no powers of N_c since meson masses and momenta scale as N_c^0 . For reasons that will presently become transparent, let us refer to the above as “naive” N_c power counting.

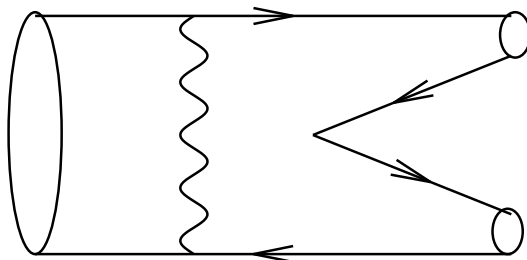


FIG. 5a. Electroweak “exchange” (E) parton diagram.

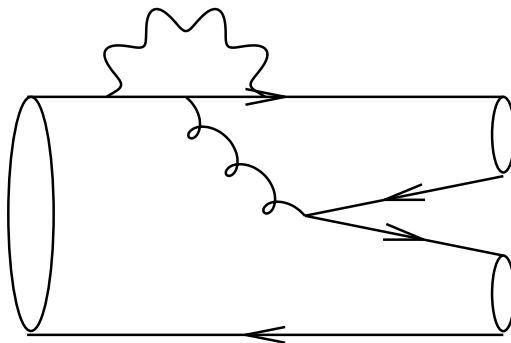


FIG. 5b. “Penguin” (P) parton diagram.

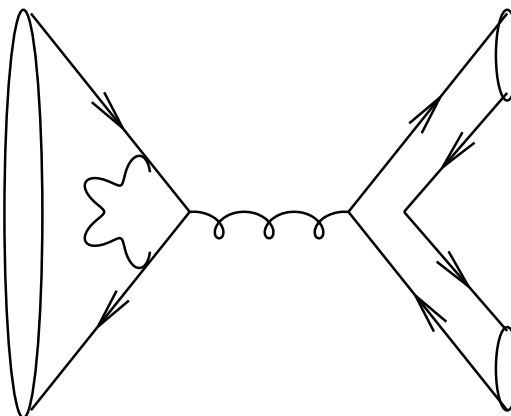


FIG. 5c. “Penguin annihilation” (PA) parton diagram. Since the initial and final states are color singlets, the intermediate state actually requires at least two gluons; however, the archetype presented here exhibits the same N_c counting.

Suppose, however, that a given diagram topology permits a resonant flavor-changing transition into a *single* meson, to which we may assign the label “one-meson decay.” Such diagrams clearly dominate over those of the corresponding two-meson decay by a factor of $\sqrt{N_c}$ in amplitude. Therefore, ’t Hooft model (or indeed any large N_c) studies of the two-meson decay mode for such diagrams appear doomed since the ’t Hooft model presents results only for behavior at leading order in N_c .

Nevertheless, the one-meson decay is a very strange physical process. For such a transition to occur on-shell, the final-state light-quark meson must have precisely the same mass as the initial heavy-light meson. The weak decay width as a function of M to lowest order in N_c is then a series of delta function spikes (since the strong decay widths of the light quark mesons scale as $1/N_c$), with a nonzero value if and only if M is tuned just right to produce such a light quark meson. In this picture, a continuum width appears only at relative order $(1/\sqrt{N_c})^2 = 1/N_c$, when two-body decays are permitted.

Clearly, this is an unsatisfactory physical picture. It implies that the leading behavior of the weak decay width scales as N_c^n for some integer n if M is tuned to certain special values, but scales as N_c^{n-1} otherwise. The simple large N_c diagram counting appears to have failed us.

Fortunately, it is not difficult to develop a useful and consistent physical interpretation for such situations. The salient point is to consider N_c very large but still finite, so that strong widths of light-quark mesons are not strictly zero; indeed, the usual N_c counting shows that their $O(1/N_c)$ strong widths are exactly what one obtains from strong decays into two lighter mesons. Thus, the one-meson decays may be interpreted as intermediate states in the decay of the initial heavy-light meson through a single resonance into the final two-meson state.

Effectively, in this picture one integrates out the one-particle decay resonant channels, which dominate the nonresonant two-particle weak decay widths by N_c^1 , from the hadronic Lagrangian. However, unitarity demands that the extra power of N_c must appear somewhere in the remaining degrees of freedom, and this is accomplished through Breit-Wigner resonances appearing in the two-meson continuum at points where the mass of the initial heavy-light meson and light-light resonance are equal. The single meson decays have thus achieved the same interpretation as the ρ peak in the $\pi\pi$ continuum.

Despite this natural interpretation, it is important to see explicitly that it supports the correct large N_c counting. Let us suppose that a certain class of diagrams gives a naive one-meson weak decay width of order N_c^n for certain special choices of M . The equivalent resonant two-meson decay diagram has a naive amplitude of order $N_c^{(n-1)/2}$ (and hence a naive width $O(N_c^{(n-1)})$), and includes a propagator of the form¹

$$\frac{i}{\mu_0^2 - \mu_p^2 + i\mu_p\Gamma_p}, \quad (2.1)$$

where the initial meson has mass μ_0 , and the resonance, labeled by p , has mass μ_p and strong width $\Gamma_p = O(1/N_c)$. Unless μ_0^2 is very close to μ_p^2 , the propagator is $O(N_c^0)$ and the naive large N_c counting is maintained. However, when $\mu_0^2 = \mu_p^2$ the previously suppressed factor Γ_p becomes dominant and promotes the propagator to a quantity of order N_c^1 . The question becomes, how much area lies under this Breit-Wigner? To answer this, we note that the relevant quantity in the width is the propagator squared. Since the peak is very tall and narrow, the rest of the invariant amplitude varies little over the width of the peak, and thus may be treated as an overall constant. We may then extend the limits of the integral in μ_0^2 from the immediate $O(1/N_c)$ neighborhood of μ_p^2 to all values $\mu_0^2 \in (-\infty, +\infty)$. Noting that

$$\int_{-\infty}^{+\infty} d\mu_0^2 \frac{1}{(\mu_0^2 - \mu_p^2)^2 + \mu_p^2\Gamma_p^2} = \frac{\pi}{\mu_p\Gamma_p} = O(N_c^1), \quad (2.2)$$

the total weak width becomes $O(N_c^n)$, and we see that the large N_c counting and unitarity are preserved, exactly as claimed. More precisely, if the product $f(\mu_0^2)$ of the invariant amplitude (except for the propagator), phase space and whatever measure we choose for the integration over μ_0^2 is a smooth function in the neighborhood of μ_p , then

¹In the narrow width approximation, which is automatically satisfied in large N_c QCD, it does not matter whether μ_p or μ_0 is chosen as the coefficient of Γ_p in the propagator. We have found that this statement is empirically true in our numerical simulations.

$$\int_{-\infty}^{+\infty} d\mu_0^2 \frac{f(\mu_0^2)}{(\mu_0^2 - \mu_p^2)^2 + \mu_p^2 \Gamma_p^2} \approx \frac{\pi f(\mu_p^2)}{\mu_p \Gamma_p} = O(N_c^1). \quad (2.3)$$

It follows that the N_c counting for two-meson decay diagrams must be modified when it is possible within the topology class to have a final state consisting of a sole color-singlet $q\bar{q}$ pair. The A and E diagrams, and those subsets of P and PA diagrams singled out above, satisfy these criteria. In such cases, the width is promoted by one power of N_c over the result of naive power counting. We obtain finally the large N_c hierarchy for diagram topologies summarized in Table 1.

N_c^2	N_c^1	N_c^0	N_c^{-1}	N_c^{-2}
A_R	T	P_R, E_R	C	PA_R

Table 1. Large N_c dependence of two-body meson decay widths from all quark diagram topologies. A subscript R indicates that the counting is enhanced by N_c^1 relative to naive counting by the presence of resonant intermediate states.

We see that the A diagram actually dominates over the T diagram studied in Ref. [1] by one power of N_c , precisely because resonance intermediates enhance the former and not the latter. However, in order for both diagrams to appear in a single process, certain restrictions on the flavors of quarks in the mesons must be imposed. This assignment must be performed with some care, because in the general case one may have to deal with the statistics of identical mesons. In order to base our conclusions on as simple a system as possible, in the present work we have chosen flavors so that such identical final-state mesons do not occur. In terms of the labels in the T diagram of Figs. 6a and the A diagram of 6b, we choose parton 1 to be the heavy quark “b” of mass M , partons 3 and 4 to refer to identical light quarks, and 2, 3 (= 4), and 5 to be quarks degenerate with mass m but of different flavors. In terms perhaps more familiar, this means that a “ \bar{B} ” meson with flavor content $(b\bar{u})$ decays to two “pion” excitations with flavors $(u'\bar{u})$ and $(d\bar{u}')$, where the u , d , and hypothetical u' quarks are degenerate in mass. Similar assignments may be used to permit certain topologies and forbid others.

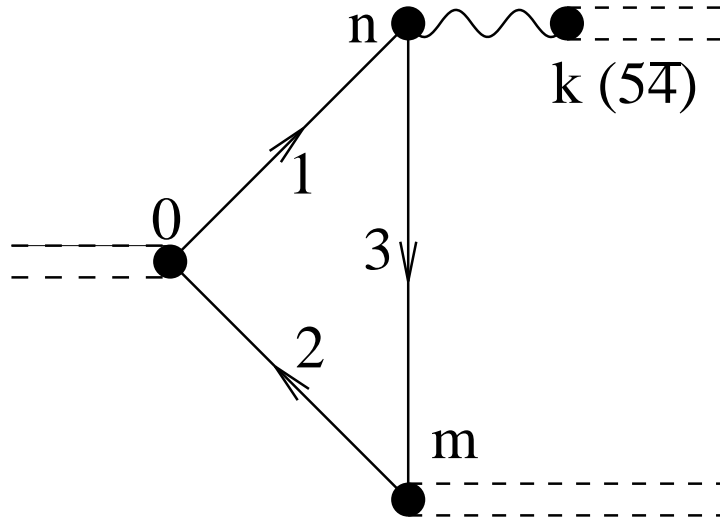


FIG. 6a. Diagram for “tree” (T) meson exclusive decay. Numbers indicate quark labels used in the text (except 0 , which refers to the ground-state “ \bar{B} ” meson), while letters indicate the eigenvalue index of meson resonances. One can also consider contact-type diagrams, in which the point labeled by n is not coupled to a resonance.

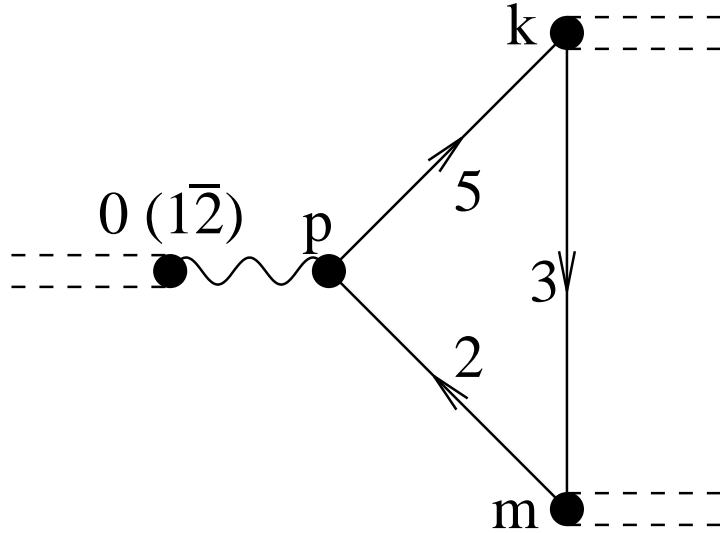


FIG. 6b. Diagram for “annihilation” (A) meson exclusive decay. Numbers indicate quark labels used in the text (except 0 , which refers to the ground-state “ \bar{B} ” meson), while letters indicate the eigenvalue index of meson resonances.

III. THE 'T HOOFT MODEL AND ANNIHILATION DIAGRAMS

A review of the application of the 't Hooft model and a description of the interesting physical peculiarities of 1+1 dimensions appears in Ref. [1]. Here we reprise only those properties essential to understanding the exceptional features of our results presented below.

The 't Hooft model is defined as $SU(N_c)$ Yang-Mills theory in 1+1 spacetime dimensions with both adjoint (gluon) and fundamental (quark) degrees of freedom in the limit of infinite group rank $N_c - 1$. This definition leads to a theory in which those Feynman diagrams with leading dependence in N_c may be summed explicitly to give closed-form expressions that are numerically, if not analytically, soluble. The archetype of these expressions is the solution for the two-point irreducible Green function, the 't Hooft equation:

$$\mu_n^2 \phi_n^{M\bar{m}}(x) = \left(\frac{M_R^2}{x} + \frac{m_R^2}{1-x} \right) \phi_n^{M\bar{m}}(x) - \int_0^1 dy \phi_n^{M\bar{m}}(y) \text{Pr} \frac{1}{(y-x)^2}, \quad (3.1)$$

where ϕ_n is the n th meson eigenfunction for a quark-antiquark pair of masses M, m , while μ is the meson mass eigenvalue, x is the fraction of the meson momentum carried by the quark in light-cone coordinates, and R indicates quark mass renormalization:

$$m_a^2 \rightarrow m_{a,R}^2 \equiv m_a^2 - g^2 N_c / 2\pi. \quad (3.2)$$

Note that gauge couplings in 1+1 dimensions have units of $(\text{mass})^1$, and recall the usual 't Hooft scaling of the strong coupling $g \propto 1/\sqrt{N_c}$. From (3.2) it then follows that $g^2 N_c / 2\pi$ serves as the natural unit of mass in the 't Hooft model, and this redefinition has already been used in Eq. (3.1). Indeed, this scale serves much the same purpose in 1+1 as Λ_{QCD} in 3+1, in that heavy quark scaling properties set in for quark masses a few times $g\sqrt{N_c}/2\pi$ [14–16].

Meson wavefunction solutions to the 't Hooft equation are either pseudoscalars or scalars, since rotations do not exist in one spatial dimension except in the residual form of spatial inversion.

That three-point 't Hooft model Green functions may be expressed in terms of two-point functions was first shown by Einhorn [17], with various generalizations demonstrated by Grinstein and Mende [15,16]. The method [18] of numerically solving the 't Hooft equation is discussed in Sec. VI, and described in detail in [1].

The most remarkable characteristic distinct to 1+1 physics exhibited by these calculations is that two-particle phase space actually becomes singular as $1/|\mathbf{p}|$ when the threshold $|\mathbf{p}| = 0$ is approached, where $|\mathbf{p}|$ is the CM spatial momentum of either outgoing meson. Nevertheless, these turn out to be rather weak square root singularities in the heavy quark mass M and therefore have pronounced effects on the width only at points over a relatively small measure in M . The corresponding familiar 3+1 expression, on the other hand, is proportional to $|\mathbf{p}|^1$ and thus vanishes at threshold.

Of much greater numerical relevance in any number of dimensions are the Breit-Wigner lineshapes produced by resonant intermediate states. As discussed in Sec. II, such resonances enhance the width by a full factor of N_c^1 for the A but not the T diagram, and therefore were not an issue in Ref. [1]. Since explicit factors of N_c no longer appear simply as a single overall coefficient in the width, one must choose a particular value for N_c in order to obtain numerical results. Quark-hadron duality should then be studied by taking N_c as large as numerically feasible; we return to a discussion of this point in Sec. VI.

IV. PARTONIC WIDTHS

The computation of the inclusive width for the decay of a heavy-light meson via the annihilation diagram at the Born level is fairly straightforward, and may be accomplished through two complementary approaches, each of which has its own advantages.

The quark Hamiltonian used for this calculation is given by

$$\mathcal{H} = G\Delta_{\mu\nu} [\bar{q}_2\gamma^\mu (c_V + c_A\gamma_5) b] [\bar{q}_5\gamma^\nu (c_V + c_A\gamma_5) q_2], \quad (4.1)$$

where

$$\Delta_{\mu\nu} = g_{\mu\nu} + \xi(p)p_\mu p_\nu \quad (4.2)$$

is the tensor structure of the weak interaction propagator with momentum transfer p . If one adopts notation analogous to that of the Standard Model, then in unitary gauge, such that charged Higgs bosons become irrelevant,

$$\xi = -1/M_W^2. \quad (4.3)$$

Similarly,

$$G = 2\sqrt{2}G_F \frac{M_W^2}{M_W^2 - p^2} V_{21}V_{25}^*, \quad (4.4)$$

where $G_F/\sqrt{2} = g_2^2/8M_W^2$ as usual. To complete the analogy, in the usual $V - A$ theory one would have $c_V = -c_A = 1/2$, but we leave these as free parameters.

The partonic calculation of the width must incorporate the annihilation of the initial meson as well as the production of final-state free quarks. Rather than decomposing the initial meson into a quark-antiquark pair free but correlated in such a way as to guarantee the desired total quantum numbers, we include the full meson coupling through

$$\langle 0 | c_V V^\mu + c_A A^\mu | n \rangle = (c_V \epsilon^{\mu\nu} + c_A g^{\mu\nu}) f_n p_\nu, \quad (4.5)$$

where $V^\mu = \bar{q}\gamma^\mu q$, $A^\mu = \bar{q}\gamma^\mu\gamma_5 q = \epsilon^{\mu\nu}V_\nu$, $\epsilon_{01} = +1$ and f_n is the decay constant of meson n . In the 't Hooft model

$$f_n = \sqrt{\frac{N_c}{\pi}} c_n \equiv \sqrt{\frac{N_c}{\pi}} \int_0^1 dx \phi_n(x). \quad (4.6)$$

The first computational approach evaluates the amplitude directly obtained from the diagram Fig. 3, where the quark-antiquark pair created by the weak current is represented by free spinors, and the on-shell process has $p^2 = \mu_0^2$. Using the Dirac equation and the 1+1 identity $\gamma^\mu\gamma_5 = \epsilon^{\mu\nu}\gamma_\nu$, one obtains

$$\mathcal{M}_A = -2\sqrt{\frac{N_c}{\pi}} G c_0 m \left[c_V^2 - c_A^2 (1 + \xi\mu_0^2) \right] [\bar{u}_5\gamma_5 v_2]. \quad (4.7)$$

The width is given by

$$\Gamma = \frac{1}{4\mu_0^2|\mathbf{p}|} |\mathcal{M}_A|^2. \quad (4.8)$$

Including a factor N_c for outgoing quarks and $1/\sqrt{N_c}$ for normalizing them into a color singlet, one obtains

$$\Gamma_{\text{part}} = N_c^2 G^2 \left[c_V^2 - c_A^2 (1 + \xi \mu_0^2) \right]^2 \frac{2m^2 c_0^2}{\pi \sqrt{\mu_0^2 - 4m^2}}. \quad (4.9)$$

It is interesting to note that the rate vanishes in the limit of massless light quarks. This follows trivially from the observation that in the $m \rightarrow 0$ chiral limit both vector and axial-vector currents (of light quarks) are conserved. Since for large N_c the A amplitude factorizes, one must contract the vector index in Eq. (4.5) with that of the current producing the quarks. Contraction with p_μ corresponds to taking the divergence of the currents, while contraction with $\epsilon_{\mu\nu} p^\nu$ corresponds to first exchanging the role of vector and axial-vector currents, and then taking the divergence. Incidentally, this argument also applies in 3+1 dimensions.

Since the decay constant $f_0 \propto c_0$ scales as $1/\sqrt{M}$ [15] and $\mu_0 \propto M$ as $M \rightarrow \infty$, the asymptotic M behavior of the annihilation diagram width Γ_{part} is $1/M^2$. This is to be contrasted with the tree diagram asymptotic width [1], which grows as M^1 .

The second computational approach evaluates the width by calculating the loop integral in Fig. 4b and then using unitarity to cut the diagram and reveal the on-shell result. Assuming that each quark has a nonzero value of some conserved quantum number such as electric charge, at most one of the two diagrams in Fig. 4b can occur in a given physical process. In the present case, it is the first diagram, which has external quark-antiquark pair 1,2 and internal quark-antiquark pair 5,2.

Standard techniques show that the inclusive width to any final states X in D spacetime dimensions is given by

$$\Gamma(\bar{B} \rightarrow X) = \frac{1}{M} \text{Im} i \int d^D x \langle \bar{B} | T \mathcal{H}^\dagger(x) \mathcal{H}(0) | \bar{B} \rangle, \quad (4.10)$$

so that one requires only (one-half of) the discontinuity in the imaginary part of the loop diagram, which begins at values of energy where on-shell intermediate states appear. The factorized four-quark operator in \mathcal{H} is used to annihilate and create a \bar{B} meson, as is again quantified by Eq. (4.5), leaving a vacuum amplitude of the product of two currents. Such factorization is a consequence of large N_c . Retaining only the internal quarks and their couplings to the weak current, one obtains for the diagram

$$\begin{aligned} & \left(-\frac{iN_c}{\pi} \right) (c_V g^\mu{}_\rho + c_A \epsilon^\mu{}_\rho) (c_V g^\nu{}_\sigma + c_A \epsilon^\nu{}_\sigma) (g^{\rho\sigma} - p^\rho p^\sigma / p^2) \\ & \cdot \left[1 - \frac{4m^2}{p^2} \frac{1}{\sqrt{4m^2/p^2 - 1}} \tan^{-1} \frac{1}{\sqrt{4m^2/p^2 - 1}} \right]. \end{aligned} \quad (4.11)$$

The discontinuity of the bracketed quantity across the cut for $p^2 \geq 4m^2$ is given by

$$\frac{4m^2}{p^2} \frac{1}{\sqrt{1 - 4m^2/p^2}}. \quad (4.12)$$

The external couplings and weak current propagators are given by

$$-G^2 f_0^2 p^\tau p^\omega [c_V \epsilon^\kappa_\tau + c_A g^\kappa_\tau] [c_V \epsilon^\lambda_\omega + c_A g^\lambda_\omega] [g_{\mu\kappa} + \xi p_\mu p_\kappa] [g_{\nu\lambda} + \xi p_\nu p_\lambda]. \quad (4.13)$$

Substituting into (4.10) the expression (4.13) contracted with (4.11) using the discontinuity in (4.12), and finally replacing f_0 using (4.6), one again obtains the partonic rate (4.9). In all subsequent expressions, we take $\xi = 0$, corresponding to $M_W \rightarrow \infty$.

Once this computation is phrased in terms of the vacuum amplitude of the product of two currents, one is tempted to replace the product of two currents by an OPE. However, this procedure is poorly justified, if at all, since the momentum across the currents, p , is neither in the deep Euclidean region (where the OPE is systematic) nor is it integrated over a region in such a way that the contour of integration can be deformed so that it lies (mostly) in the deep Euclidean region. The physical quantity of interest is the rate at a given heavy meson mass, so that $p^2 = \mu_0^2$ is timelike. One can, however, consider integrating the rate over the variable p^2 . Then, as in the more familiar case of $e^+e^- \rightarrow$ hadrons, the contour can be deformed and the integral is dominated by the leading term in the OPE. Putting aside the question of physical utility of this exercise (in reality, unfortunately, we cannot vary the mass of the \bar{B} meson), in the 't Hooft model it has long been known [10,17] that this leading order OPE result is reproduced by the sum over intermediate resonant states; for clarity, we demonstrate this result in the current notation below. Large N_c counting dictates that only single intermediate states contribute. If global duality (that is, including integration over p^2) is operative in the rate for annihilation decays, it must be through some nontrivial interplay between these resonances and the inclusion of widths for internal meson propagators in the exclusive rates, as discussed in Sec. II.

In the 't Hooft model one may explicitly check duality for the vacuum amplitude of the product of two currents in the limit of p^2 large and in any complex direction except along the positive real axis (where meson poles occur). In fact, this limit was considered first by Callan, Coote, and Gross [10], with a number of refinements by Einhorn [17], but it is instructive to see how the calculation proceeds when arbitrary combinations of vectorlike currents are included. Defining $\tilde{p}^\mu = \epsilon^{\mu\nu} p_\nu$ and using $\epsilon^{\mu\kappa} \epsilon^\nu_\kappa = -g^{\mu\nu}$, the $p^2 \gg m^2$ limit of the loop expression (4.11) reads

$$\left(-\frac{iN_c}{\pi}\right) \left\{ (c_V^2 - c_A^2) g^{\mu\nu} - \frac{1}{p^2} (c_V^2 p^\mu p^\nu + c_A^2 \tilde{p}^\mu \tilde{p}^\nu) - \frac{c_V c_A}{p^2} (p^\mu \tilde{p}^\nu + \tilde{p}^\mu p^\nu) \right\}. \quad (4.14)$$

On the other hand, the hadronic vertex is defined by Eq. (4.5), and so the loop written in terms of resonance contributions reads

$$(c_A \epsilon^\mu_\tau + c_A g^\mu_\tau) (c_V \epsilon^\nu_\omega + c_A g^\nu_\omega) p^\tau p^\omega \sum_n \frac{i f_n^2}{p^2 - \mu_n^2}. \quad (4.15)$$

As $p^2 \rightarrow$ complex ∞ , the sum becomes

$$\frac{i}{p^2} \sum_n f_n^2 = \frac{iN_c}{\pi p^2} \sum_n c_n^2 = \frac{iN_c}{\pi p^2}, \quad (4.16)$$

which uses the definition (4.6) and the completeness relation

$$\sum_n \phi_n(x)\phi_n(y) = \delta(x - y). \quad (4.17)$$

In this limit, (4.15) contracts to

$$\left(+\frac{iN_c}{\pi} \right) \left\{ c_V^2 \frac{\tilde{p}^\mu \tilde{p}^\nu}{p^2} + c_A^2 \frac{p^\mu p^\nu}{p^2} + \frac{c_V c_A}{p^2} (\tilde{p}^\mu p^\nu + p^\mu \tilde{p}^\nu) \right\}. \quad (4.18)$$

To see that (4.14) and (4.18) are equal requires one to recognize the following (equivalent) tensor identities, which hold in 1+1:

$$\begin{aligned} p^\mu p^\nu - p^2 g^{\mu\nu} &= \tilde{p}^\mu \tilde{p}^\nu, \\ \tilde{p}^\mu \tilde{p}^\nu + p^2 g^{\mu\nu} &= p^\mu p^\nu. \end{aligned} \quad (4.19)$$

It goes without saying that a demonstration of the validity of an OPE for hadronic widths in the real world of four dimensions and three colors would be much more subtle, as one loses some simplifying elements such as factorization.

If it nevertheless can be shown that the nonleptonic expansion admits a well-defined OPE, then the diagrams of Fig. 4b enter as effective four-quark operators of the form

$$\mathcal{O}_A = \bar{b}\Gamma^\mu q_2 \bar{q}_2 \Gamma_\mu b, \quad (4.20)$$

where Γ^μ represents the vectorlike (V^μ and A^μ) Lorentz structures. In contrast, the T diagram arises from cutting the loop diagram of Fig. 4a, and enters the effective OPE through the leading operator $\mathcal{O}_T = \bar{b}b$. Since fermion fields in D spacetime dimensions have engineering dimension $M^{(D-1)/2}$, by naive power counting the A diagram width in 1+1 might be expected to be only $1/M$ suppressed compared to that of the T diagram. Schematically, the OPE-like expression for the width reads

$$\Gamma(\bar{B} \rightarrow X) \sim G_F^2 M^{2D-4} \left\{ \langle \bar{B} | \bar{b}b | \bar{B} \rangle + \dots + \frac{1}{M^{D-1}} \langle \bar{B} | \bar{b}\Gamma^\mu q_2 \bar{q}_2 \Gamma_\mu b | \bar{B} \rangle + \dots \right\}, \quad (4.21)$$

where the ellipses indicate subleading terms for both the T and A contributions, and numerous overall coefficients as well as perturbative short-distance corrections have been suppressed for simplicity. The overall mass factor is obtained by noting that the mass dimension of G_F is M^{2-D} , while the \bar{B} bra and ket are normalized to $2M$ particles per unit volume and thus have mass dimension $M^{(1-D/2)}$. Each term in the braces has dimension M^1 .

However, this reasoning does not take into account the light quark mass suppression induced by taking the divergence of the light quark current. One obtains an additional suppression m^2/M^2 as discussed above, and thus (4.21) does indeed predict $\Gamma_A \propto 1/M^2$ as $M \rightarrow \infty$ in 1+1, in agreement with (4.9).

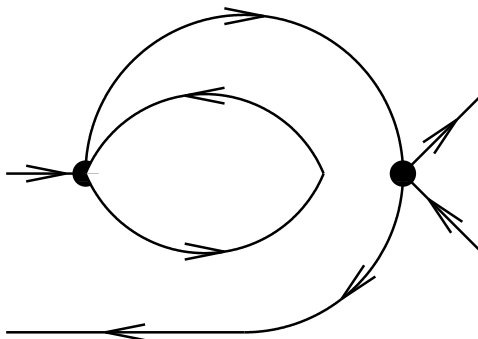


FIG. 7. Feynman diagram topology for the interference between A and T amplitudes.

An important point to note is the absence of interference effects between A and T amplitudes in the total width predicted by the OPE-like expansion, Eq. (4.21). The diagram in Fig. 7 would contribute to such an interference effect, but is of order N_c^1 rather than $N_c^{3/2}$ as suggested by Table 1. The absence of interference in the OPE method is not by itself proof of failure of the method since there could be cancellations among the exclusive channels that effectively cancel the interference effects.

V. HADRONIC WIDTHS IN THE 'T HOOFT MODEL

In Ref. [1] the amplitude for each allowed exclusive channel proceeding through the T diagram of Fig. 6a was computed in terms of various sums and overlaps of 't Hooft model wavefunctions. Such an expression, Eq. (5.8) or (5.18) in that work, represents the exact nonperturbative calculation of the invariant amplitude within the 't Hooft universe of 1+1 spacetime dimensions and large N_c .

The analogous calculation for the A diagram of Fig. 6b is almost identical, and essentially amounts to a reassignment of indices, as expected from crossing symmetry.² The expressions in terms of form factors are very similar to those for the T diagram, and so we instead present only the result for the invariant amplitude. As before, $\mathbf{0}$ refers to the initial ground state ($1\bar{2}$) meson, and is now directly coupled to the flavor-changing current. The light meson at the other end of this current, labeled by \mathbf{p} , has quantum numbers ($5\bar{2}$); \mathbf{m} as before refers to the final-state ($3\bar{2}$) meson, and \mathbf{k} (which is no longer coupled to the flavor-changing current), has quantum numbers ($5\bar{3}$): Recall the statement in Sec. II that, in order to have both T and A diagrams, we require quarks 3 and 4 to be identical. The kinematic variable, now defined by $\omega \equiv q_-/p_-$, is given for this diagram by

$$\omega(p^2) = \frac{1}{2} \left[1 + \left(\frac{\mu_k^2 - \mu_m^2}{p^2} \right) - \sqrt{1 - 2 \left(\frac{\mu_k^2 + \mu_m^2}{p^2} \right) + \left(\frac{\mu_k^2 - \mu_m^2}{p^2} \right)^2} \right]. \quad (5.1)$$

²Since $\mu_0^2 > (\mu_k + \mu_m)^2$ for all on-shell processes, it follows that ω defined here in (5.1) always lies in $[0, 1]$, and one may directly use the analogue of (5.8) in [1] rather than worrying about “back-solving” or “contact terms” as described in the previous work.

Here we see that the relevant threshold is that of $\mathbf{0} \rightarrow \mathbf{m}\mathbf{k}$, *i.e.*, $p^2 = (\mu_k + \mu_m)^2$. The invariant amplitude for states above this threshold is given by

$$\mathcal{M}_A = Gc_0 \sqrt{\frac{N_c}{\pi}} \sum_p \left[[(c_V^2 - c_A^2)(1 + (-1)^p)] - \xi p^2 c_A [(c_V + c_A)(-1)^p - (c_V - c_A)] \right] \cdot \frac{c_p \mu_p^2}{(p^2 - \mu_p^2 + i\mu_p \Gamma_p)} F_{pkm}(\omega_0), \quad (5.2)$$

where now the on-shell process has $p^2 = \mu_0^2$, $\omega_0 \equiv \omega(p^2 = \mu_0^2)$, and the triple overlap is given by

$$F_{pkm}(\omega) \equiv \left[\frac{1}{1 - \omega} \int_0^\omega dv \phi_p^{5\bar{2}}(v) \phi_k^{5\bar{3}}\left(\frac{v}{\omega}\right) \Phi_m^{3\bar{2}}\left(\frac{v - \omega}{1 - \omega}\right) - \frac{1}{\omega} \int_\omega^1 dv \phi_p^{5\bar{2}}(v) \Phi_k^{5\bar{3}}\left(\frac{v}{\omega}\right) \phi_m^{3\bar{2}}\left(\frac{v - \omega}{1 - \omega}\right) \right], \quad (5.3)$$

where the meson-quark vertex function is defined by

$$\Phi_n^{M\bar{m}}(z) = \int_0^1 dy \phi_n^{M\bar{m}}(y) \Pr \frac{1}{(y - z)^2}. \quad (5.4)$$

Note also the presence of the partial width Γ_p for light-light meson \mathbf{p} strong decay into mesons \mathbf{k} and \mathbf{m} . As argued in the Sec. II, such an inclusion is essential to give a consistent large N_c power counting for the two-meson weak decay diagram. Explicitly,

$$\Gamma_p(\omega_p) = \frac{2\pi}{N_c \mu_p} \sum_{k,m} \left[(\mu_p^2)^2 - 2\mu_p^2 (\mu_k^2 + \mu_m^2) + (\mu_k^2 - \mu_m^2)^2 \right]^{-1/2} |F_{pkm}(\omega_p)|^2, \quad (5.5)$$

where, using (5.1), $\omega_p \equiv \omega(p^2 = \mu_p^2)$.

The total rate Γ_{had} for the A diagram is then obtained by squaring (5.2), inserting the result into (4.8), and summing over all allowed final states \mathbf{k} and \mathbf{m} . This value is to be compared with the Born term expression (4.9) as a test of quark-hadron duality.

One may also consider direct numerical comparisons between the T diagram total hadronic rate exhibited in Fig. 4 of [1] and Γ_{had} computed here; the correct procedure to follow in this case is somewhat ambiguous, since the former rate is of order N_c^1 , while the latter integrates to order N_c^2 when resonant contributions are taken into account. Therefore, if one works only in the strict large N_c limit, the T diagram is infinitely small compared to the A diagram. However, while the 't Hooft model is of course only exactly true when $N_c \rightarrow \infty$, this limit is believed to survive the inclusion of $O(1/N_c)$ corrections [10]. Moreover, since numerous studies in the literature show that the phenomenological predictions of the large N_c expansion survive even for N_c as small as 3, we suppose that a quantitative comparison between the T and A widths has merit even for small N_c .

VI. RESULTS AND DISCUSSION

The 't Hooft equation is solved numerically by means of the Mulhopp technique [18], by which the integral expression (3.1) is converted to an equivalent eigenvector equation

amenable to solution using computers. The results presented here were computed with a basis set of $K = 200$ eigenfunctions. As a check that this set is sufficiently large, the computation was repeated using of $K = 50$. Figure 8 shows the ratio of the total width, solely from the annihilation topology, computed for $K = 50$ to that for $K = 200$, in the case of (a) $N_c = 10$, and (b) $N_c = 1$. In both cases the ratio of the Gaussian-smearred widths [see below, Eq. (6.2)] is also shown, with a Gaussian width of (a) $\Delta M = 1.2$ and (b) $\Delta M = 0.4$, in mass units of $g\sqrt{N_c/2\pi}$. In either case the difference for widths is never more than 30%, while for the average width it is never more than 10%, and less than 5% in the region $M > 10$.

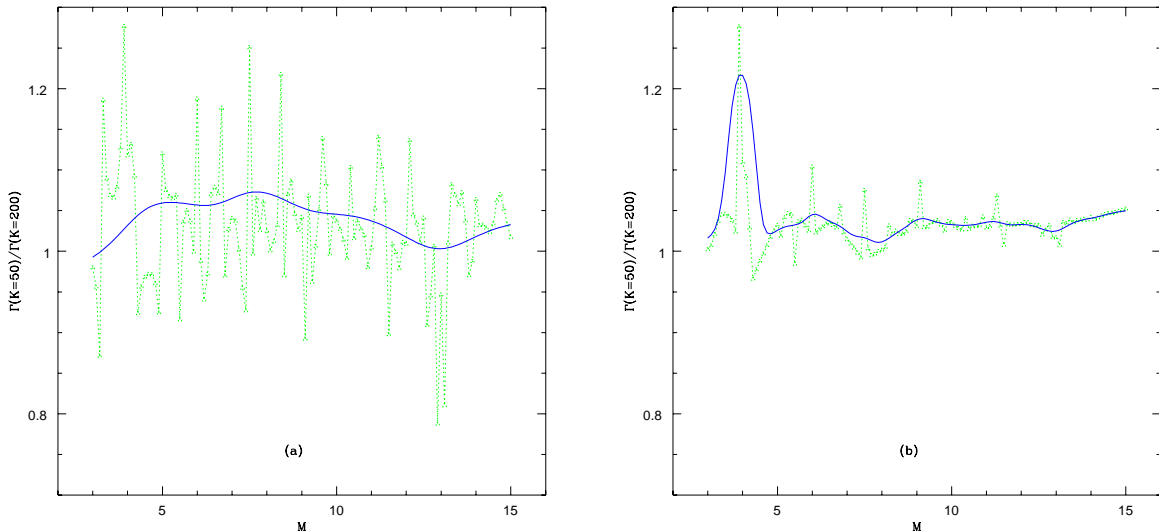


FIG. 8. Ratio of the total width, solely from the annihilation topology, computed for $K = 50$ to that for $K = 200$, in the case of (a) $N_c = 10$, and (b) $N_c = 1$. In both cases the ratio of the Gaussian-smearred widths is also shown, with a Gaussian width of $\Delta M = 1.2$ in (a) and $\Delta M = 0.4$ in (b). The unit of mass here and in all subsequent figures is $g\sqrt{N_c/2\pi}$.

In all calculations we choose a single fixed value of mass common to all the light quarks, $m = 0.56$. The range of M over which calculation of $\Gamma_{\text{had}}(M)$ is feasible is limited primarily by the rapidly increasing number of exclusive channels open to the decay of the \bar{B} meson as M increases, and the concomitant computing time required for the necessary integral overlaps. In practice, we limit our studies to the range from $M = 2.28$ (the lightest heavy quark mass that creates a \bar{B} with just enough mass to decay to two ground-state light-light mesons) to $M = 15.00$ (at which point almost 150 exclusive channels are open) in units of $g\sqrt{N_c/2\pi}$.

Incidentally, it is known that the standard Mulhopp technique leads to inaccurate 't Hooft wavefunctions when $m \ll 1$. In Ref. [20], an improved version of the Mulhopp method is developed, which does a much better job calculating the wavefunctions near $x = 0$ and 1 when m is small. One may question whether $m = 0.56$ is large enough that our results, computed by the standard technique, are reliable. We find that computing with the technique of [20] tends to change the results by only a few parts in 10^4 . Therefore, we are

confident in presenting numerical results below that use the standard Multihopp technique.

The Breit-Wigner resonances, which become infinitely tall and narrow as $N_c \rightarrow \infty$, present much more severe singularities in Γ_{had} than the phase space singularities discussed in Sec. III. Indeed, without proper regularization they are non-integrable, and therefore no amount of averaging, or “smearing,” could produce a finite result. One must include the $O(1/N_c)$ strong widths of the meson resonances coupled to the weak current, as discussed in Sec. II.

The strong widths are interesting in their own right. The exact expression for the widths is given in Eq. (5.5). In Fig. 9 we show the results of this calculation for meson excitation numbers from 0 to 155, along with a fit function

$$\Gamma_n^{\text{fit}} = 22 \times \frac{0.44}{\pi^2 N_c} \sqrt{n-1}. \quad (6.1)$$

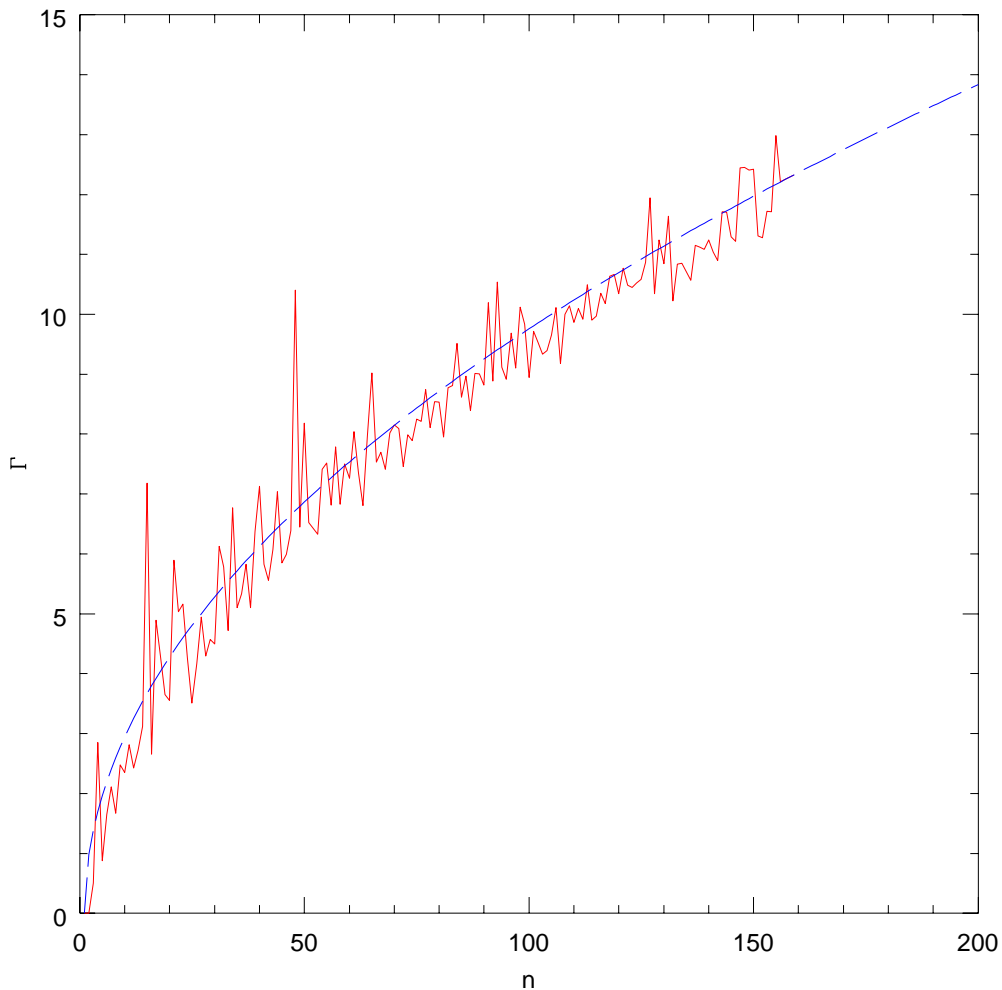


FIG. 9. Meson strong decay widths in units of $g\sqrt{N_c/2\pi} \cdot 1/N_c$ as computed via (5.5). The smooth dashed curve is the fit function (6.1).

The coefficient is written in this peculiar format in order to facilitate comparison with the results of Blok *et al.* [19], whose best fit appears to be a factor 22 smaller than ours. There are two differences between their calculation and ours. First, they work with massless light quarks $m = 0$ so that they may use analytic expressions for 't Hooft wavefunctions. Second, their light quarks, unlike ours, appear to be chosen as indistinguishable, leading to a different pattern of interference terms in the invariant amplitudes. When strong widths for $n > 155$ are needed, we use the fit function Γ_n^{fit} .

In the present case in which strong widths can become important, factors of N_c no longer appear simply as an overall coefficient, as was the case in [1]. We are thus forced to choose particular values of N_c in order to obtain numerical results. The ideal, of course, is to choose N_c as large as possible in order to approach the results of the exact 't Hooft model. However, such a choice makes the Breit-Wigners taller, narrower, and thus harder to average over M , so that obtaining a smooth result for comparison with the one computed perturbatively is more difficult. In particular, one is forced to choose the range ΔM over which the averaging function has support to be larger and larger in order to obtain at last a smooth result for $\Gamma_{\text{had}}^{\text{avg}}$.

The averaging, or “smearing,” of $\Gamma_{\text{had}}(M) \rightarrow \Gamma_{\text{had}}^{\text{avg}}(M)$ in the heavy quark mass M is carried out here by multiplying $\Gamma_{\text{had}}(M)$ at a series of points M_0 over the range of M by a suitably chosen smearing function, and then normalizing by the area under this function. In practice we use a Gaussian of width $\Delta M/\sqrt{2}$:

$$\Gamma_{\text{had}}^{\text{avg}}(M) = \frac{\sum_{M_0} \exp\left[-\frac{(M-M_0)^2}{(\Delta M)^2}\right] \Gamma_{\text{had}}(M)}{\sum_{M_0} \exp\left[-\frac{(M-M_0)^2}{(\Delta M)^2}\right]}, \quad (6.2)$$

and the points M and M_0 are chosen at intervals of 0.1 mass units. It should be pointed out that this smearing produces a small spurious result at the edges of the fitting range if the function to be smeared has a nonzero derivative (apart from noise in the function) at these points. For example, suppose one smears a linearly decreasing function near its endpoint. The smearing function of course samples only points to the left of the endpoint, where the function is uniformly larger than it is at the endpoint itself, and so the smeared result is slightly higher than expected. One of many cures is to compare two curves smeared in the same way, which produces the same spurious effect in both, and so such curves may be compared directly.

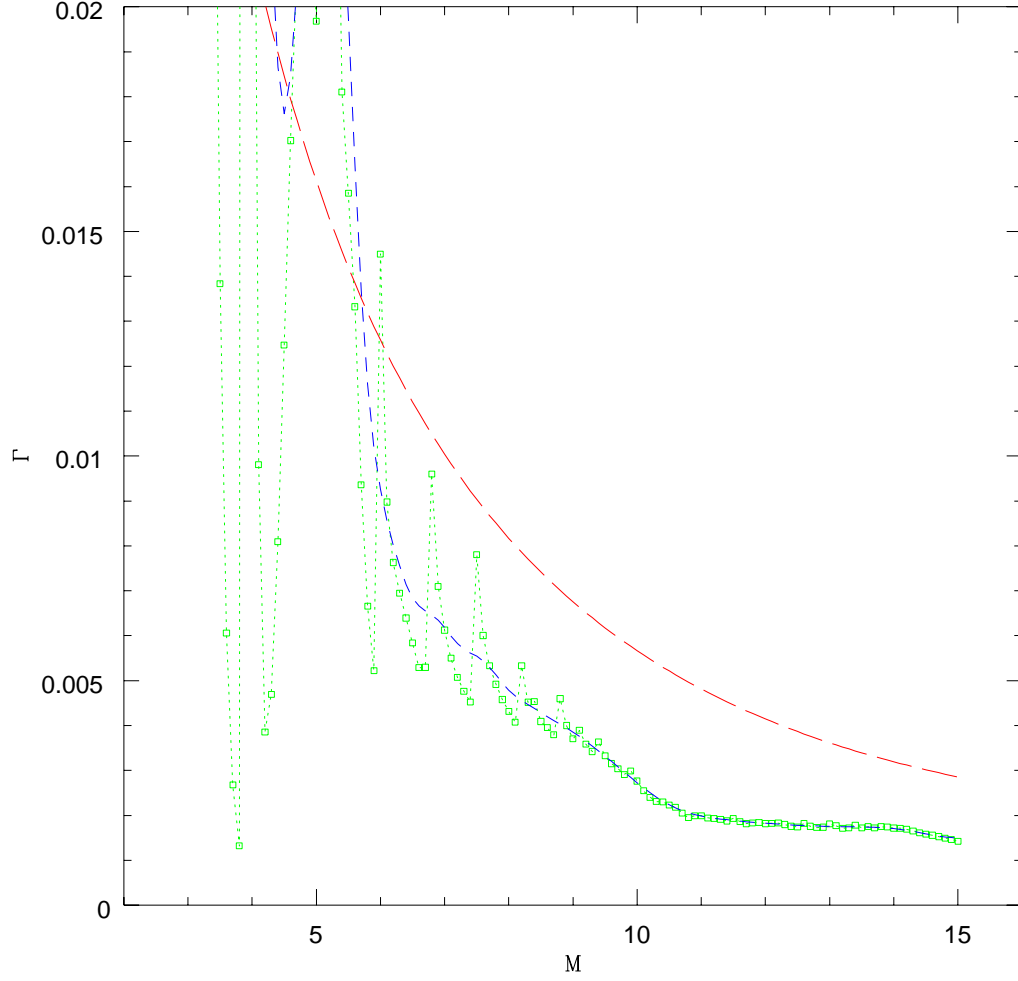


FIG. 10. Total annihilation width of the “ \bar{B} ” meson as a function of the heavy quark mass M , for $N_c = 1$ (dotted line). The smeared width defined in Eq. (6.2) is shown in short dashes, and was computed using $\Delta M = 0.4$. The partonic width is shown in long dashes. Units of the widths here and below are $N_c^1 G^2 (c_V^2 - c_A^2)^2$.

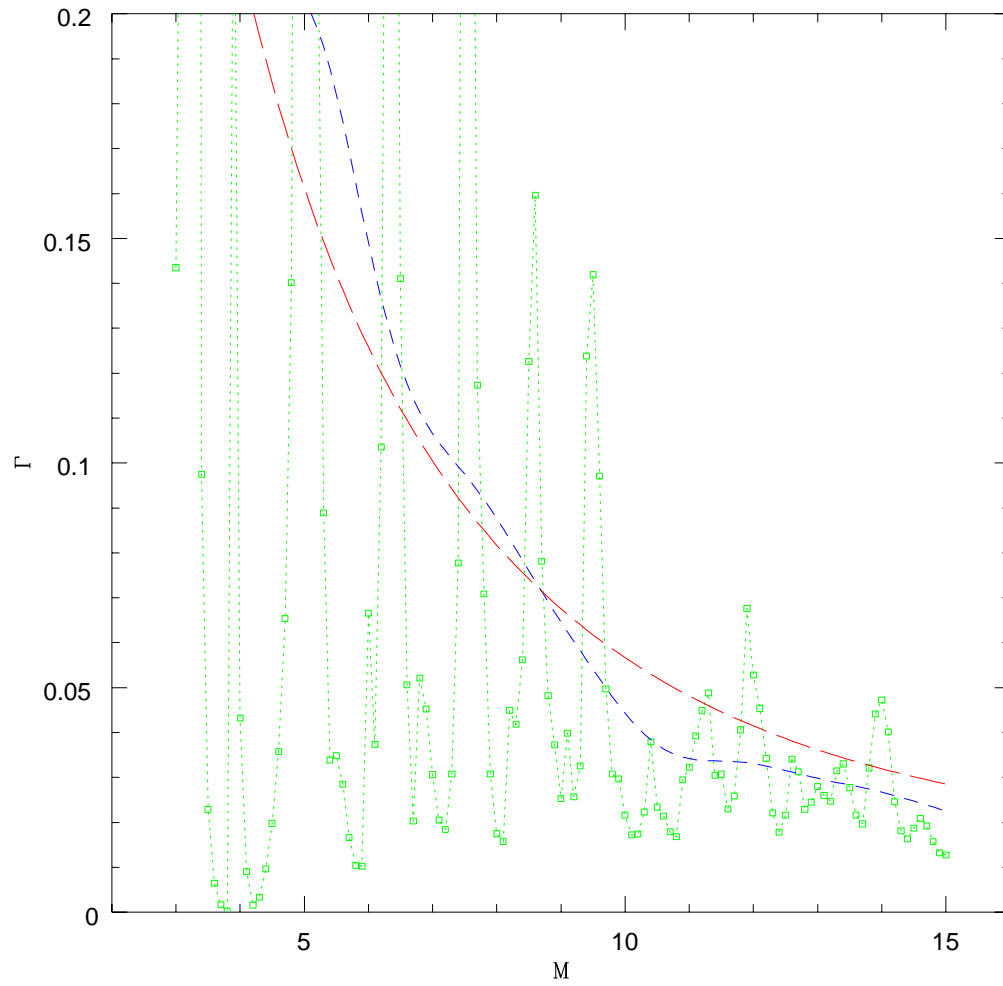


FIG. 11. As in Fig. 10, but with $N_c = 10$ and $\Delta M = 1.2$.

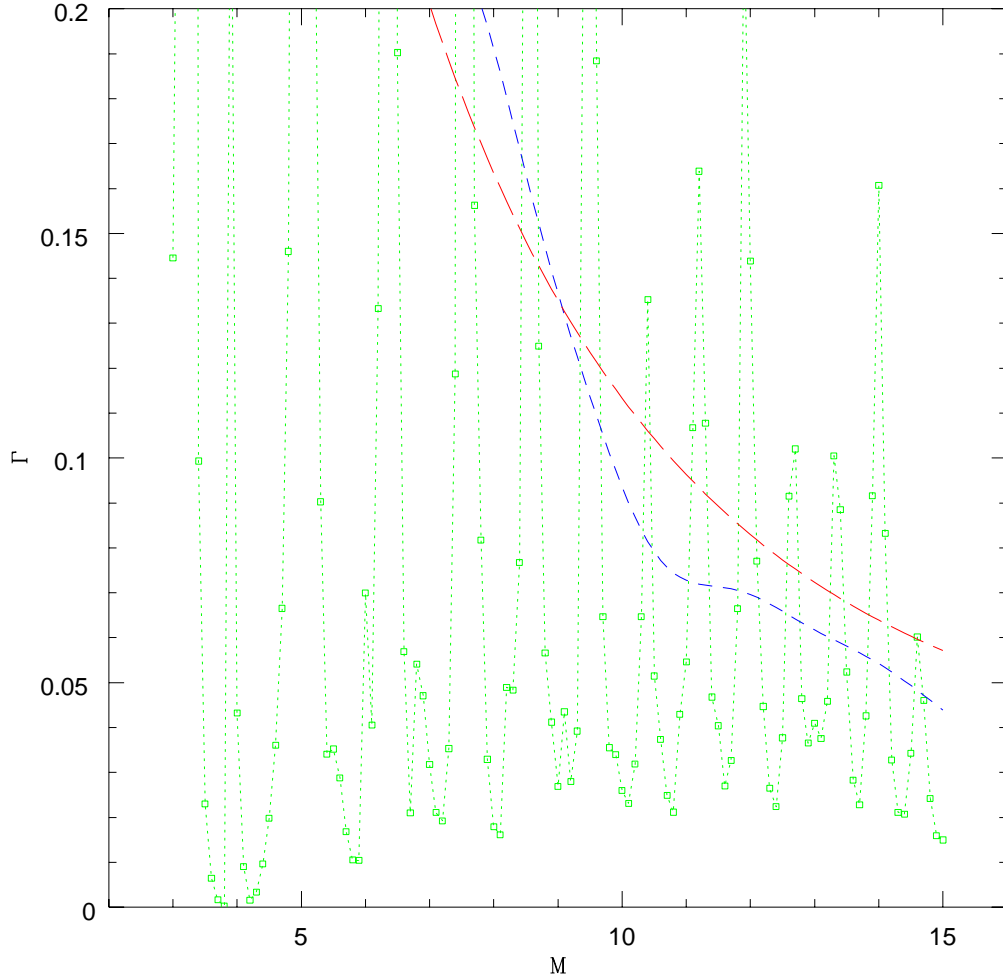


FIG. 12. As in Fig. 10, but with $N_c = 20$ and $\Delta M = 1.2$.

The main results of this paper are exhibited in Figs. 10–13, which we now discuss. Figures 10–12 show in dotted lines the total annihilation width of the “ \bar{B} ” meson as a function of the heavy quark mass M . Widths are presented in units of $N_c^1 G^2 (c_V^2 - c_A^2)^2$. The computation was carried out at the points shown as small squares, and the dotted lines connect between them, to guide the eye. Widths for the internal resonances have been included, and so the plots depend on N_c , with $N_c = 1, 10$ and 20 for Figs. 10, 11, and 12 respectively. Also, in all three figures we show in short dashes the Gaussian-smearred width, taking $\Delta M = 0.4, 1.2$ and 1.2 for Figs. 10, 11, and 12 respectively. We see that the larger the width of the internal resonances (that is, the smaller N_c), the smoother the behavior of Γ_{had} , so that ΔM as small as 0.4 is sufficient to smooth out the $N_c = 1$ case, whereas for $N_c = 20$ the larger value $\Delta M = 1.2$ had to be used. In each figure the partonic width is displayed in long dashes.

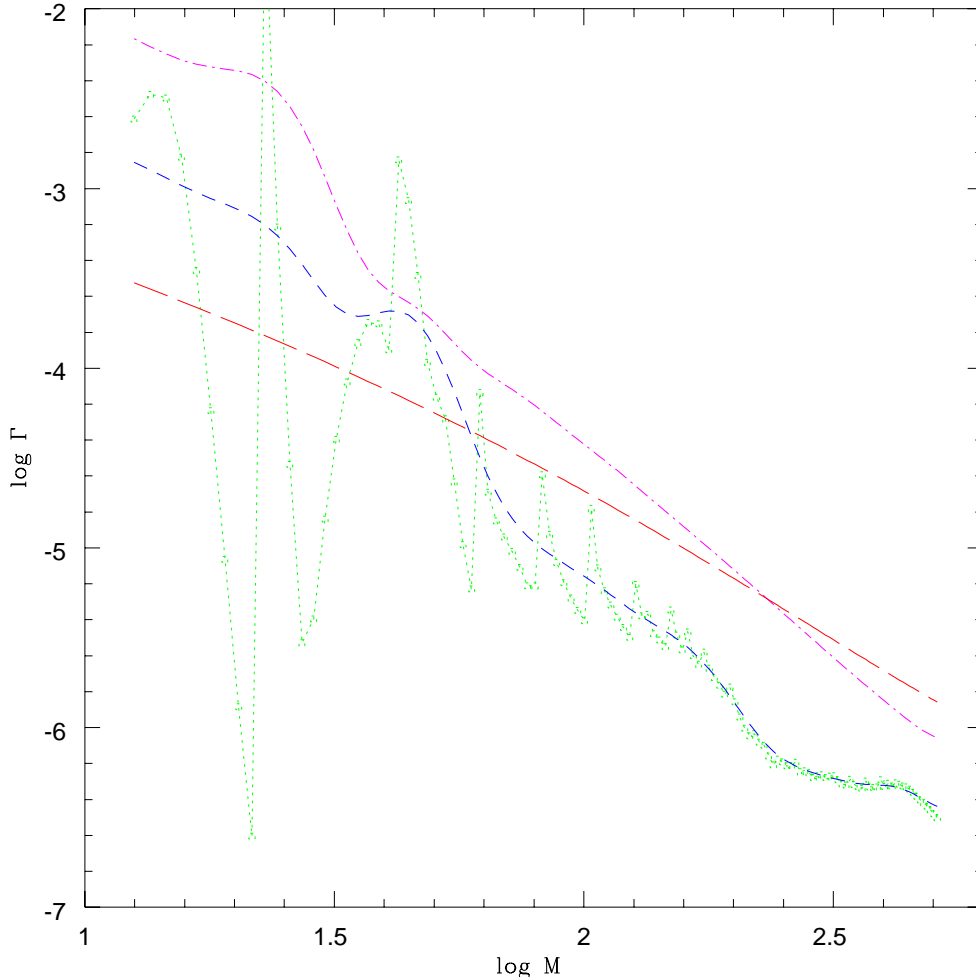


FIG. 13. Log-log plot of the total annihilation width of the “ \bar{B} ” meson as a function of the heavy quark mass M , for $N_c = 1$ (dotted line). The smeared width defined in Eq. (6.2) is shown in short dashes, and was computed using $\Delta M = 0.4$. The partonic width is shown in long dashes. Also shown, in dash-dot-dash, is the Gaussian-smeared result that uses the model of Eq. (6.1) for the strong widths of the internal resonances.

It is apparent that there is a large discrepancy between the actual widths and the partonic ones. The disagreement remains after smearing. We may now ask whether the disagreement is a correction that decreases as a particular power of M . Figure 13 displays the same information as Fig. 10, but in log-log format. Also shown, in dash-dot-dash, is the Gaussian-smeared result that uses the model of Eq. (6.1) for the strong widths of the internal resonances. Even though Γ_{part} and $\Gamma_{\text{had}}^{\text{avg}}$ achieve somewhat better relative agreement as N_c is increased, we see that $\Gamma_{\text{had}}^{\text{avg}}$ is not without structure, indicating that for this type of process the onset of the asymptotic large M limit is very delayed. This is similar to what occurs for the decay constant f_B ; the combination $\sqrt{M}f_B$ is known to have large $1/M$ and $1/M^2$ corrections [15]. We have refrained from displaying a plot of $L = \log(\Gamma_{\text{had}}^{\text{avg}}/\Gamma_{\text{part}} - 1)$, which at large M would display the leading power correction M^{-p} as the slope of L versus $\log M$.

The problem in doing so is that, as discussed, it is clear that even at these large values of M the asymptotic behavior is not in sight. It is interesting to note that the dash-dot-dash line is smooth and its slope disagrees sharply with that of Γ_{part} .

Finally, regarding the question of a direct comparison of T versus A widths, we remind the reader that different N_c behavior between the two widths means that, for N_c sufficiently large, the A diagram dominates. However, there are two additional effects that must be taken into account. The first is that asymptotically, $\Gamma_T \propto M$ but $\Gamma_A \propto 1/M^2$; thus for large M and N_c fixed, one expects $\Gamma_A/\Gamma_T \ll 1$. Much more interesting are the true dynamical effects obtained from the exactly computed matrix elements and Breit-Wigner resonances in the A diagram. Once the result for Γ_T given in Fig. 4 of [1] is properly normalized³, one still finds that Γ_T is much larger than Γ_A , even for fairly large N_c and fairly small M . For example, for $N_c = 10$ and $M = 5$ (see Fig. 11) one finds $\Gamma_T/\Gamma_A > 3$. It appears that, in the context of the 't Hooft model generalized to finite N_c , one must choose N_c exceptionally large before finding values of M for which $\Gamma_T \approx \Gamma_A$.

VII. CONCLUSIONS

We have studied the annihilation decays of heavy “ \bar{B} ” mesons in the 't Hooft model as a function of the heavy quark mass M for fixed light quark mass m . In the strict large N_c limit the hadronic width solely due to annihilation decays, $\Gamma_{\text{had}} = \Gamma(\bar{B})$, displays resonant structure from intermediate light mesons. For almost all values of M the partonic width, Γ_{part} , which displays no structure, is at strong variance with the exact width $\Gamma(\bar{B})$. A comparison with a smeared version of $\Gamma(\bar{B})$ is not possible since the resonant singularities in $\Gamma(\bar{B})$ are non-integrable.

It seems plausible, however, that for large but finite N_c and at large enough M a smeared version of $\Gamma(\bar{B})$ may agree with Γ_{part} . For finite N_c the hadronic widths of the resonances in $\Gamma(\bar{B})$ must be included and make it possible to study the smeared version of $\Gamma(\bar{B})$, $\Gamma_{\text{had}}^{\text{avg}}$. Moreover, the leading dependences on N_c of $\Gamma_{\text{had}}^{\text{avg}}$ and Γ_{part} coincide. However, our numerical study shows that even at masses as large as $M = 15$ in units of $g\sqrt{N_c/2\pi}$, $\Gamma_{\text{had}}^{\text{avg}}$ and Γ_{part} disagree significantly. Although increasing N_c improves the relative agreement somewhat, the improvement is not strong enough to claim the onset of asymptotic scaling, even by $M = 15$.

Our analysis does not conclusively show the breakdown of duality for annihilation decays of heavy mesons. But it seems clear that if duality is operative asymptotically, it must be that asymptotia is much delayed for these types of decays.

Acknowledgments

RFL is pleased to acknowledge enlightening discussions with Nathan Isgur. This work is

³In the notation of this paper, the overall coefficient of the older figure is $N_c G^2 (c_V^2 - c_A^2)^2 / \pi$. One must divide Γ_T by this extra π to obtain numerical comparisons. There are also different CKM elements, $V_{31}V_{35}^*$ for T and $V_{21}V_{25}^*$ for A, that we take equal for comparison purposes.

supported by the Department of Energy under contract Nos. DOE-FG03-97ER40506 and DE-AC05-84ER40150.

APPENDIX A: VAN ROYEN-WEISSKOPF RELATION IN ARBITRARY DIMENSIONS

It is interesting to consider the generalization of the van Royen-Weisskopf relation [21], which connects the meson decay constant to the value of the meson wavefunction at zero quark separation, and was therefore implicitly used in the original naive argument in Sec. I that the annihilation diagram is suppressed compared to the tree diagram. This relation is proved using nonrelativistic constituent quarks within the meson; nevertheless, one may consider its generalization to arbitrary N_c and D spacetime dimensions, in which it reads

$$f_B^2 = \frac{4N_c |\psi(0)|^2}{M + m}. \quad (\text{A1})$$

Note particularly that D only enters this expression implicitly in $\psi(0)$. The explicit factor of N_c from f_B^2 is in fact the source of the enhancement of the A width to the T width. To proceed, we require a model for the wavefunction, for which we choose

$$\psi(\mathbf{r}) = R(r)Y_{00}(\Omega) = Ne^{-\mu r}Y_{00}, \quad (\text{A2})$$

where μ is a typical hadronic mass scale, the D -dimensional spherical harmonic is given by

$$|Y_{00}(\Omega)|^2 = \frac{1}{\int d\Omega} = \frac{\Gamma((D-1)/2)}{2\pi^{(D-1)/2}}, \quad (\text{A3})$$

and $N^2 = (2\mu)^{D-1}/\Gamma(D-1)$. We then have

$$f_B^2 = \frac{4N_c}{M + m} \cdot \frac{\Gamma((D-1)/2)}{2\pi^{(D-1)/2}} \cdot \frac{(2\mu)^{D-1}}{\Gamma(D-1)}. \quad (\text{A4})$$

Note that the mass dimension of f_B is $M^{D/2-1}$, as can also be shown directly from its definition (4.5) as a matrix element.

In the context of dimensional regularization, the factor appearing with the inclusion of each additional loop is $(4\pi)^{-D/2}$. We must also, according to the arguments of Sec. I, divide out powers of m_B ($= M + m$ in this model) to obtain a dimensionless ratio. The relevant ratio between the A and T diagram widths in this simple model is thus given by

$$(4\pi)^{D/2} \frac{f_B^2}{m_B^{D-2}} = N_c \left(\frac{\mu}{M + m} \right)^{D-1} \cdot 4^D \sqrt{\pi} \frac{\Gamma((D-1)/2)}{\Gamma(D-1)}. \quad (\text{A5})$$

Removing the explicit N_c and the mass ratio, the remaining D -dependent coefficient actually reaches a maximum for $D = 9$. We see that even in this simple model — no dynamics, not even a helicity suppression factor, has been included — tells us the ratio between the A and T diagrams depends sensitively on interplay between the value of N_c , the quark masses and interaction energies, and the number of spacetime dimensions.

REFERENCES

- [1] B. Grinstein and R. F. Lebed, *Phys. Rev. D* **57**, 1366 (1998).
- [2] K. Wilson, *Phys. Rev.* **179**, 1499 (1969) and *Phys. Rev. D* **3**, 1818 (1971);
W. Zimmerman, *Ann. Phys. (New York)* **77**, 536 and 570, 1973.
- [3] H. Georgi and H. D. Politzer, *Phys. Rev. D* **9**, 416 (1974);
D. J. Gross and F. Wilczek, *Phys. Rev. D* **9**, 920 (1974).
- [4] M. A. Shifman, A. I. Vainshtein, and V. I. Zakharov, *Nucl. Phys. B* **147**, 385 (1979);
ibid., 448.
- [5] J. Chay, H. Georgi, and B. Grinstein, *Phys. Lett. B* **247**, 399 (1990).
- [6] I. I. Bigi, B. Blok, M. A. Shifman, N. G. Uraltsev, and A. Vainshtein, in *Proceedings of The Fermilab Meeting: DPF 92*, Edited by Carl H. Albright, Peter H. Kasper, Rajendran Raja, and John Yoh. (World Scientific, River Edge, N.J., 1993), p. 610.
- [7] ALEPH Collaboration (R. Barate *et al.*), *Eur. Phys. C* **2**, 197 (1998);
ALEPH Collaboration (R. Barate *et al.*), Preprint No. CERN PPE/97 157 (unpublished);
Particle Data Group (R. M. Barnett *et al.*), *Phys. Rev. D* **54**, 1 (1996).
- [8] M. Neubert and C. T. Sachrajda, *Nucl. Phys. B* **483**, 339 (1997).
- [9] G. 't Hooft, *Nucl. Phys. B* **75**, 461 (1974).
- [10] C. G. Callan, Jr., N. Coote, and D. J. Gross, *Phys. Rev. D* **13**, 1649 (1976).
- [11] G. 't Hooft, *Nucl. Phys. B* **72**, 461 (1974).
- [12] E. Witten, *Nucl. Phys. B* **160**, 57 (1979) provides an excellent review of these properties.
- [13] M. Gronau, O. F. Hernández, D. London, and J. L. Rosner, *Phys. Rev. D* **50**, 4529 (1994).
- [14] R. L. Jaffe and P. F. Mende, *Nucl. Phys. B* **369**, 189 (1992).
- [15] B. Grinstein and P. F. Mende, *Phys. Rev. Lett.* **69**, 1018 (1992).
- [16] B. Grinstein and P. F. Mende, *Nucl. Phys. B* **425**, 451 (1994).
- [17] M. B. Einhorn, *Phys. Rev. D* **14**, 3451 (1976).
- [18] A. J. Hanson, R. D. Peccei, and M. K. Prasad, *Nucl. Phys. B* **121**, 477 (1977); K. Karamchetti, *Principles of Ideal-Fluid Aerodynamics*, John Wiley & Sons, New York, 1966.
- [19] B. Blok, M. Shifman, and D.-X. Zhang, *Phys. Rev. D* **57**, 2691 (1998);
B. Blok, *Nucl. Phys. Proc. Suppl.* **64**, 481 (1998).
- [20] R. C. Brower, W. L. Spence, and J. H. Weis, *Phys. Rev. D* **19**, 3024 (1979).
- [21] R. van Royen and V. F. Weisskopf, *Nuovo Cimento* **50A**, 617 (1967).

Figure Captions

FIG. 1. The (color-unsuppressed) “tree” (T) parton diagram for the decay of one meson into two mesons. Ovals indicate the binding of partons into hadrons.

FIG. 2. The “color-suppressed” (C) parton diagram for the decay of one meson into two mesons. Ovals indicate the binding of partons into hadrons.

FIG. 3. The “annihilation” (A) parton diagram for the decay of one meson into two mesons. Ovals indicate the binding of partons into hadrons.

FIG. 4*a*. Diagram giving rise to the “tree” amplitude of Fig. 1 upon a vertical cut through the center (application of unitarity). The vertex blobs indicate W exchange.

FIG. 4*b*. Diagrams giving rise to the “annihilation” amplitude of Fig. 3 upon a vertical cut through the center (application of unitarity). The vertex blobs indicate W exchange. Strongly produced $q\bar{q}$ pairs are not drawn here for simplicity.

FIG. 5*a*. Electroweak “exchange” (E) parton diagram.

FIG. 5*b*. “Penguin” (P) parton diagram.

FIG. 5*c*. “Penguin annihilation” (PA) parton diagram. Since the initial and final states are color singlets, the intermediate state actually requires at least two gluons; however, the archetype presented here exhibits the same N_c counting.

FIG. 6*a*. Diagram for “tree” (T) meson exclusive decay. Numbers indicate quark labels used in the text (except $\mathbf{0}$, which refers to the ground-state “ \bar{B} ” meson), while letters indicate the eigenvalue index of meson resonances. One can also consider contact-type diagrams, in which the point labeled by \mathbf{n} is not coupled to a resonance.

FIG. 6*b*. Diagram for “annihilation” (A) meson exclusive decay. Numbers indicate quark labels used in the text (except $\mathbf{0}$, which refers to the ground-state “ \bar{B} ” meson), while letters indicate the eigenvalue index of meson resonances. One can also consider contact-type diagrams, in which the point labeled by \mathbf{p} is not coupled to a resonance.

FIG. 7. Feynman diagram topology for the interference between A and T amplitudes.

FIG. 8. Ratio of the total width, solely from the annihilation topology, computed for $K = 50$ to that for $K = 200$, in the case of (a) $N_c = 10$, and (b) $N_c = 1$. In both cases the ratio of the Gaussian-smearred widths is also shown, with a Gaussian width of $\Delta M = 1.2$ in (a) and $\Delta M = 0.4$ in (b). The unit of mass here and in all subsequent figures is $g\sqrt{N_c/2\pi}$.

FIG. 9. Meson strong decay widths in units of $g\sqrt{N_c/2\pi} \cdot 1/N_c$ as computed via (5.5). The smooth dashed curve is the fit function (6.1).

FIG. 10. Total annihilation width of the “ \bar{B} ” meson as a function of the heavy quark mass M , for $N_c = 1$ (dotted line). The smeared width defined in Eq. (6.2) is shown in short dashes, and was computed using $\Delta M = 0.4$. The partonic width is shown in long dashes. Units of the widths here and below are $N_c^1 G^2 (c_V^2 - c_A^2)^2$.

FIG. 11. As in Fig. 10, but with $N_c = 10$ and $\Delta M = 1.2$.

FIG. 12. As in Fig. 10, but with $N_c = 20$ and $\Delta M = 1.2$.

FIG. 13. Log-log plot of the total annihilation width of the “ \bar{B} ” meson as a function of the heavy quark mass M , for $N_c = 1$ (dotted line). The smeared width defined in Eq. (6.2) is shown in short dashes, and was computed using $\Delta M = 0.4$. The partonic width is shown in long dashes. Also shown, in dash-dot-dash, is the Gaussian-smearred result that uses the model of Eq. (6.1) for the strong widths of the internal resonances.